SCATTERING MATRIX CALCULATION OF HIGHER ORDER MODES AND SENSITIVITY TO CAVITY FABRICATION ERRORS FOR THE ILC SUPERCONDUCTING CAVITIES

I. Shinton and R.M. Jones; The University of Manchester, Manchester M13 9PL, UK
and Cockcroft Institute of Science and Technology, Daresbury, Cheshire WA4 4AD, UK

Abstract

A cascaded scattering matrix approach is used to determine the eigenmodes and driven modes in the main linac cavities of the ILC. This approach is used to compute higher order e.m. modes in the baseline configuration, and high gradient alternative configurations. We present results on three cavity designs: TESLA, Cornell University's re-entrant and, KEK's "Ichiro". This approach allows realistic experimental errors to be incorporated in the studies in an efficient manner and allows several cavities to be modelled. Implications of indentations in the cavity on the modal properties of the structure are presented.

INTRODUCTION

Several cavity structures exist for the proposed ILC linac alternate design including the prototype higher gradient of Cornell University's re-entrant and KEK's "Ichiro" or low loss cavity design. In a practical accelerating structure machining and alignment errors will exist; the effect of these realistic errors needs to be carefully considered and there is a need to be able to accurately model the higher order deflecting modes in the main linacs of the ILC en masse in which their influence on wake-fields and beam dynamics are ascertained. Here as part of this paper we present an initial study into the sensitivity of the three cavity designs to the effects of a symmetrically applied perturbation. However, it important to note that even with parallel FEM code [1] an accurate model of the main linacs of the ILC will require substantial resources and time to compute. Moreover, the inclusion of realistic defects and misalignments into the baseline configuration will prove time consuming as it will potentially require remeshing of the problem and will not readily lend itself to the introduction of a distribution of errors. An alternative to a direct numerical approach is to use the relatively mature concept of the globalised scattering (S) matrix technique [2] which focuses on the modes of interest.

The generalised scattering matrix technique has been shown to be capable of accurately simulating structures [2], [3], [4]. The technique is very efficient and can readily incorporate misalignments and cavity perturbations into the calculation. There are a number of methods that can be found throughout the literature, the form used in this paper is that of [2]. We present the initial findings for cavity perturbations applied to a 9-cell structure using a generalised scattering matrix technique. This analysis has been restricted to try and better understand the complex nature of perturbations on an accelerating structure. The possibility of using symmetrically applied perturbations to eliminate trapped modes located too far from the couplers to be removed was tentatively investigated. Similar approaches by which deliberate perturbations are introduced to try and prevent beam breakup have appeared in the literature [5].

We focus our analysis on dipole modes because for small offsets in the beam from the electrical centre or small cell perturbations [6] these modes dominate the beam dynamics. The impact of these modes is described in terms of kick factors [7]. The distribution of these eigenmodes and kick factors are important as an adequate knowledge of them will allow beam dynamics simulations on the emittance of the beam down 11 km of the entire linac.

All references to either the Cornell re-entrant [8] or KEK's "Ichiro" [9], [10] designs relate only to specifically chosen designs investigated within this paper. The geometry of the cavity tangent of α=75.75° optimised for a maximum GR/Q for the Cornell re-entrant [8] and the K. Saito January 2007 design [9], [10] were used in all the calculations conducted in this paper.

Unless otherwise specified, all the eigen modal calculations were conducted using HFSS v8.5 employing linear FEM elements and the mesh was adaptively refined until a tolerance of 0.005% was achieved, which corresponds to a tolerance of ±0.5MHz. All the S matrices required for the cascading calculations were carried out using HFSS v10; where a driven modal solution was sought in which quadratic FEM elements were used and the mesh was adaptively refined until an overall accuracy below 0.01% was obtained for the resulting S parameters followed by a frequency sweep from 1 to 4.5GHz conducted in linear steps of 0.01GHz. All the S matrices, cascaded, were renormalized within HFSS v10 using an impedance factor of 50 Ohms; in which the unit cell structure is taken from iris to iris. In all driven modal solutions conducted a finite copper conductivity was assigned to all metallic surface [3]. The dipole and sextupole modes, calculated either in an eigen or driven modal solution, for all the symmetrical structures were modelled using a quarter of the geometry and E and H symmetry planes.

Benchmarking against Slater's theorem

Slater's theorem [11] provides an approximate analytical form for the frequency shifts due to small perturbations in the cavity geometry. The main advantage of such a scheme is that once an accurate numerical simulation of a cavity structure has been preformed a

straightforward and rigorous application of Slater's theorem provides a reliable estimate of the frequency shift. This scheme requires little in the way of computation resources. We apply Slater's theorem to verify the simulations performed herein.

The benchmarking problem of a TESLA [7] middle cell with four symmetrically placed perturbations to simulate frequency shifts expected from typical experimental errors was investigated. As the perturbed structure is a symmetric one only a quarter of the geometry needs to be simulated. An isoparametric drawing of the simulated structure is presented in Fig. 1, in which the perturbation is located upon the equator radius at an equal distance between the symmetry planes. This perturbation shall be referred to henceforth as a "slice", because it is effectively a removal of material at a distance perpendicular from the surface of the equatorial radius, which henceforth will be referred to as the slice size. As this perturbation is located on an electric boundary Slater's theorem is simplified to accounting for only the case of an electric mirror perturbation. The numerical eigen calculations were conducted using HFSS v8.5 with periodic boundary conditions applied at the ports and which all simulations were run until a tolerance of 0.005% was achieved. Slater's theorem was applied to an unperturbed cavity using the internal calculator within HFSS v8.5, in which a virtual object was included for the purpose of representing the perturbation. A Table comparing the frequency shifts calculated by numerical means to those calculated by the application of Slater's theorem are shown in Table 1 for various slice sizes.

All the results depicted in Table 1 are accurate to ±0.5MHz, due to the tolerance of HFSS 8.5. Notable frequency shifts above this tolerance have been highlighted in yellow.

The numerically calculated results generated with HFSS v8.5 are in general in good agreement with those predicted from Slater's theorem. This validates the accuracy of the numerical method employed to study the effects of cavity perturbations and provides some confidence in the accuracy of the results.

It was discovered that slice sizes above 3 mm gives rise to a distortion of some of the modes of interest. These distortions correspond to a significant mode conversion. Within this paper we restrict the slices to a maximum of 3 mm and hence we are limited to the effects of perturbations on the eigen-modes.

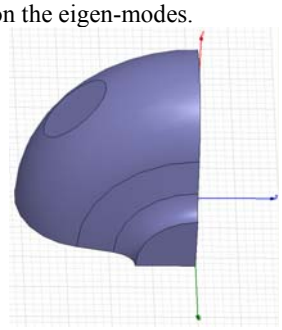

Figure 1 Isoparametric representation of a quarter of a TESLA middle cell with a 3 mm slice size perturbation applied at the equator radius.

DENTED STRUCTURE SIMULATIONS

The effect of a symmetrically placed perturbation upon the middle cell cavity designs of the TESLA [7], Cornell University's re-entrant [6] and KEK's "Ichiro" [9], [10] was investigated. The aforementioned cavity perturbation discussed in the benchmarking example was used to investigate the sensitivity of the three designs in terms of frequency shifts for various slice sizes. The results of this investigation are summarised in Table 2, in which all the results are accurate to ±0.5MHz and notable frequency shifts above this tolerance have been highlighted in yellow.

Curves comparing the three designs showing the effect of frequency shifts as a function of slice size for various bands are displayed below in Fig 2 and Fig 3, in which some of the more interesting trends displayed in Table 2 are graphically displayed.

	TESLA	SLATER	TESLA	SLATER	TESLA	SLATER
Slice: mm	1	1	2	2	3	3
Dipole band 1 shift f0	0.05	-0.01	-0.15	-0.05	0.08	-0.10
Dipole band 1 shift fpi	-0.22	-0.25	-1.13	-1.24	-2.84	-2.47
Dipole band 2 shift f0	-0.39	-0.37	-1.76	-1.59	-3.97	-3.28
Dipole band 2 shift fpi	0.06	-0.01	0.00	-0.05	-0.07	-0.10
Dipole band 3 shift f0	0.28	0.10	0.64	0.42	1.33	0.86
Dipole band 3 shift fpi	-0.04	-0.13	-0.18	-0.65	-0.98	-1.28
Dipole band 4 shift f0	-0.01	-0.13	-0.57	-0.57	-1.49	-1.22
Dipole band 4 shift fpi	0.46	0.21	1.20	0.96	1.86	1.76
Sextupole band 1 shift f0	0.12	-0.06	-0.18	-0.30	-0.62	-0.61
Sextupole band 1 shift fpi	0.21	-0.05	-0.13	-0.28	0.17	-0.42
Sextupole band 2 shift f0	-0.95	-0.79	-3.56	-3.31	-7.78	-6.76
Sextupole band 2 shift fpi	-0.90	-0.69	-3.44	-3.33	-7.90	-6.63

Table. 1 Comparison between numerically calculated frequency shifts (MHz) and those calculated by Slater's theorem for various slice size perturbations applied at the equatorial radius for four symmetrically placed slices for 0 (F0) and π (Fpi) phase modes. Notable frequency shifts are highlighted in yellow. All results are accurate to ±0.5MHz.

	TESLA	ICHIRO	CORNELL	TESLA	ICHIRO	CORNELL	TESLA	ICHIRO	CORNELL
Slice: mm	1	1	1	2	2	2	3	3	3
Dipole band 1 shift f0	0.05	-0.05	-0.01	-0.15	-0.01	0.07	0.08	-0.09	-0.31
Dipole band 1 shift fpi	-0.22	0.05	-0.09	-1.13	-0.05	-0.17	-2.84	-0.18	-0.33
Dipole band 2 shift f0	-0.39	-0.45	-0.35	-1.76	-2.12	-1.56	-3.97	-4.73	-4.25
Dipole band 2 shift fpi	0.06	-0.39	-0.46	0	-1.77	-1.38	-0.07	-3.87	-3.48
Dipole band 3 shift f0	0.28	0.42	0.21	0.64	1.37	0.58	1.33	2.94	1.61
Dipole band 3 shift fpi	-0.04	-0.56	-0.17	-0.18	-0.84	-0.31	-0.98	-1.6	-0.91
Dipole band 4 shift f0	-0.01	-0.45	-0.21	-0.57	-1.86	-1.31	-1.49	-4.04	-3.61
Dipole band 4 shift fpi	0.46	0.03	-0.44	1.2	-0.6	-0.99	1.86	-1.91	-1.78
Sextupole band 1 shift f0	0.12	-0.23	-0.17	-0.18	-0.63	-0.68	-0.62	-1.62	-1.47
Sextupole band 1 shift fpi	0.21	0.81	-0.24	-0.13	1.85	0.65	0.17	3.97	2.21
Sextupole band 2 shift f0	-0.95	-0.03	0.01	-3.56	-0.01	0.11	-7.78	-0.15	-0.1
Sextupole band 2 shift fpi	-0.9	-0.43	-0.61	-3.44	-2.48	-1.93	-7.9	-5.48	-5.07

Table. 2 Comparison of the numerically calculated frequency shifts (MHz) for three designs and for various slice size perturbations applied at the equator radius for 0 (F0) and π (Fpi) phase modes. Notable frequency shifts are highlighted in yellow. All results are accurate to ±0.5MHz.

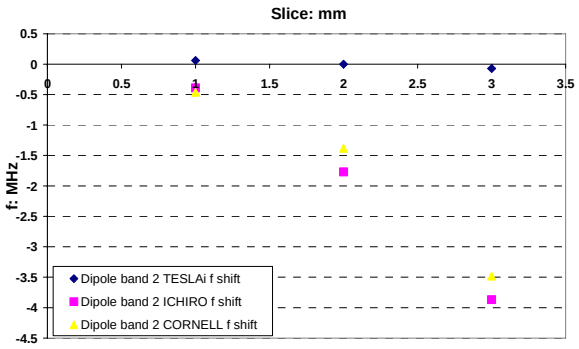

Figure 2 Frequency shifts as a function of slice size for the π phase mode of the second dipole band.

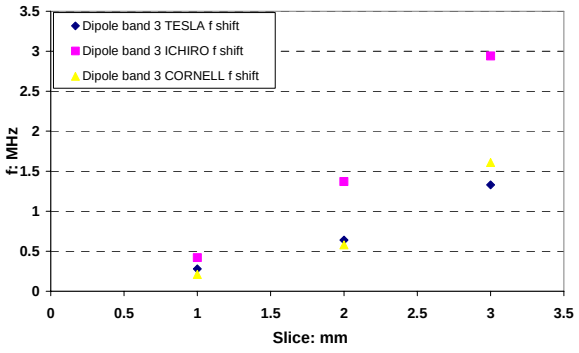

Figure 3 Frequency shifts as a function of slice size for the 0 phase mode of the third dipole band.

CASCADED SIMULATIONS WITH MACHINING ERRORS

The effect of cavity perturbations of the type considered in the preceding sections was applied to a 9-cell TESLA cavity with TTF type beam pipes [7]. This initial investigation provides a means to evaluate both the sensitivity of such a structure to perturbations as well as the possibility of using deliberately introduced perturbations to attempt to eliminate trapped modes and reduce the effect of beam breakup instabilities [5].

A generalised scattering matrix approach [2] was utilised to study these effects, as it provides a means to simulate very large amalgams of accelerating structures. However here the analysis has been restricted to a single 9-cell structure in order to reduce the complexity of the problem and to provide a better means for understanding the effects of such perturbations.

The unit cell calculations were carried out using a total of six modes per port, in which slice sizes of 1mm, 2mm and 3mm were individually applied to the middle cells only. A comparison of frequency shifts induced by various perturbations in the unit cell structures are presented in Fig 4 and Fig 5. Even though a 1 mm slice size on its own does not produce any appreciable frequency shifts (as can be seen perusing results contained in both Table 1 and Table 2) it does change the magnitude of S_{21}. A plot of the dominant S_{21} mode scattered into the third mode (sextupole), shown in Fig 5, has been illustrates that a small perturbation can effect the structure by altering the energy distributed into the various modes. Thus, a relatively small perturbation can change the mode kick factor appreciably.

Both the size of the perturbation and its location in the 9-cell structure have a noticeable effect on the cascaded S matrices. Even though the higher order multi-poles are progressively more sensitive to perturbations their effect on the beam dynamics is relatively small compared to the dominant dipole modes. In the frequency range of interest we included sextupole modes and found that they are indeed more sensitive to perturbations than dipole modes. We will focus on the dominant TE_{11} mode as it has the largest scattering coefficient.

Trapped modes which do not penetrate the higher mode coupler region will not be damped in the present superconducting cavity design. However, one possible means of removing such modes would be to deform a cell in the region of the trapped mode to shift the frequencies and mode distributions of the cells. The symmetric perturbation considered herein could be employed to this end. Any trapped mode located in the middle of the 9-cell structure will be particularly difficult to deal with as it cannot be readily removed via the couplers. In Fig, 6 curves are presented to illustrate the induced frequency shifts and alterations in the energy distribution for a 3 mm

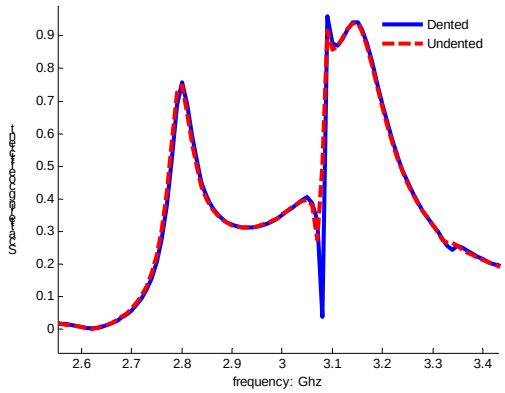

Fig. 4 Zoomed in unit cell S_{21} matrix comparison between an unperturbed structure and a perturbed structure with a slice size of 3mm for the dominant TE_{11} mode scattered into the TE_{11} mode.

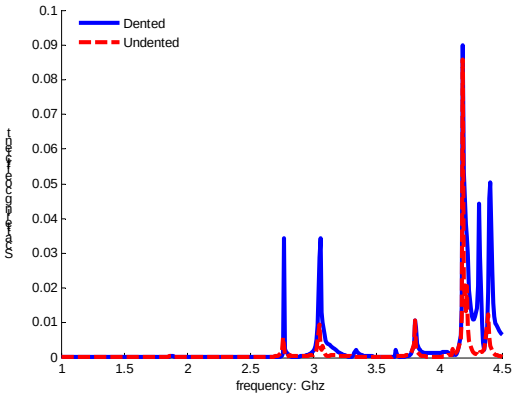

Fig. 5 Zoomed in unit cell S_{21} matrix comparison between an unperturbed structure and a perturbed structure with a slice size of 1mm for the dominant TE_{11} mode scattered into the third mode (sextupole).

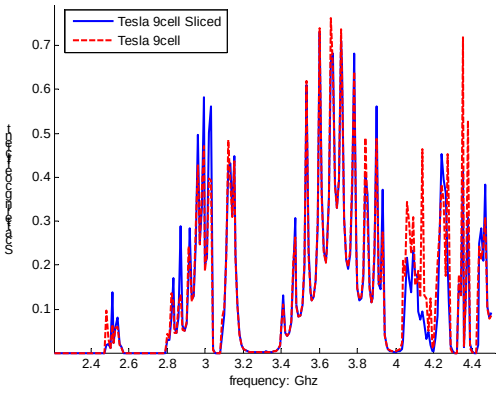

Fig 6 Zoomed in region of the generalised cascaded S_{21} matrix for a 9-cell TESLA structure comparison between an unperturbed structure and the RMS of a randomly perturbed structure for the TE11 mode scattered into the TE11 mode. Here the middle cells in the structure were randomly perturbed using slice sizes of 0mm, 1mm, 2mm and 3mm with the RMS taken for 20 different simulations.

randomly distributed slice errors. Here, we consider the dominant TE_{11} mode scattered into the TE_{11} mode. This provides an initial step towards simulation of realistic experimental errors that will be present in the fabrication of 16,000 of such cavities for the ILC.

ELECTROMAGNETIC FIELDS AND FUTURE WORK

A generalised cascaded scattering matrix by itself only gives an indication of the energy distribution within a structure, from plots of the scattering coefficients of the various elements of the S matrices the modal frequencies of a structure can be determined (from direct inspection). However in order to determine trapped and beam pipe modes the electromagnetic fields need to be derived. The electromagnetic fields are also necessary for calculating the kick factors and transverse R/Q values of an accelerating structure.

There are two basic approaches that could be employed in order to re-derive the electromagnetic fields from the cascaded S matrices. The first approach entails directly incorporating the derived S matrices as boundary conditions into a driven modal FEM scheme to recalculate the electromagnetic fields. The main advantage of such an approach would be that it is direct and the same computational mesh used in the unit cell calculations could be employed. The disadvantage with this approach is that it would require extra computation resources and time in order to re-derive the electromagnetic fields.

The second approach would be to directly employee an analytical mode match scheme to the generalised cascaded S matrices. Such an approach has been the approach of choice for cascading schemes in previously developed accelerator structures [12]. Provided enough modes are considered the method is robust, efficient and requires little in the way of computational resources. However in applying such an approach to any of the three cavity designs cavities is not a trivial matter. The mode matching process is complicated for such cavity shapes, because the propagation constant is no longer a constant with respect to the radial direction.

Once the electromagnetic field has been characterised along the axis for a specific radial offset, the kick factors and transverse R/Qs are obtained using [7]. This will enable beam dynamics issues to be investigated firstly, using a sum wake-field [3] and later with full beam dynamics tracking simulations. Additional complex phenomena [13] may also be investigated using this method. Furthermore, a more thorough perturbation investigation can be conducted, with the final aim to model a significant fraction of the accelerating modules of the ILC with realistic effects and locate potentially harmful trapped modes.

DISCUSSION

The numerical results calculated directly with HFSS v8.5 are in good agreement with those predicted by

Slater's theorem. This provides a validation of the method employed to investigate symmetrically applied cavity perturbations. A symmetrically applied perturbation was chosen to evaluate both the sensitivity of the three designs to perturbations and also to provide an initial means to investigate the effect of such perturbations upon a 9-cell structure. It was discovered that slice sizes greater than 3mm distorted the modes of interest. This provides an indication of the tolerance of such cavities to machining and alignment errors as in this case the modes are sufficiently distorted, they fail to follow the e.m. field distribution designed for the cavity. This may give rise to a finite number of insufficiently damped modes.

A number of interesting trends may be gleamed from the calculated frequency shifts in Table 2; in general it can be seen that the Cornell and Ichiro designs follow similar frequency shift trends in which it is the Ichiro design which is more sensitive to cavity perturbations of the symmetric nature discussed in the paper. The TESLA design typically follows the trends observed in the other designs in which it appears to be the least effected by symmetric cavity perturbations. However the TESLA design does significantly depart from the observed behaviour of the other cavities for several of the HOM modes (an example of which is shown in Fig 2). The effect of randomly placed perturbations on a real accelerating structure, which occurs naturally as a result of the fabrication process, is in fact beneficial. In a true idealised accelerating structure the cumulative effect of all the transverse fields acting consecutively would ultimately result in beam breakup. Detuning of the accelerating structure would then be required, as was the case for the X-band accelerating structure [12]. However the presence of machining and alignment errors (which will be present in any accelerating structure) will randomly shift the transverse modes and limit the effect of emittance dilution. Thus, it is clear that these cavities are quite sensitive to perturbation errors and thus detuning of the accelerating structure will occur naturally as a result of the fabrication process.

The perturbation study was extended to the situation of a 9-cell TESLA cavity, in which a cascading technique was employed to analyse the effects of perturbations on the structure with the possibility of using such a perturbation to eliminate trapped modes that are localised too far from the couplers to be damped adequately. A cascading technique was used for this purpose because it provides a means to simulate very large accelerating structures. The analysis was restricted to a single 9-cell structure in order to reduce the complexity of the problem and provide a better means for understanding the effects of such perturbations. Comparison of the perturbed and unperturbed unit cell S matrices displayed the expected frequency shifts predicted by the eigen modal analysis. However it was found that a small perturbation can affect the structure by altering the energy distributed into the various modes, as can be seen by referring to Fig 5 in which a 1mm slice size (a perturbation which by in itself does not cause any appreciable frequency shifts as can be seen by the results displayed in Table 2) caused energy to be distributed into some of the HOM modes (sextupole). The effect of altering the size of the perturbation produces a more striking effect in the energy distribution than the induced overall frequency shift alone, as can be seen in Fig 3. However, for slice indentation larger than 3 mm a significant mode distortion is observed.

In applying a perturbation to a 9-cell structure the placement and size of the perturbation has a significant effect on the generalised scattering matrix. The altered energy distribution of the HOM's is a somewhat random and unpredictable effect, as can be seen in the altered energy distribution in Fig 6, in which it may be noted that the 3rd and 8th dipole bands are significantly effected. The possibility of using perturbations to shift or damp the energy distributed into trapped modes was considered. However, in a realistic accelerating structure the cumulative effect of perturbations may result a complex energy distribution that will be quite different to that predicted by an idealised structure. However, modelling such perturbations will allow particularly damaging modal distributions to be predicted and the sensitivity of the cavity to errors to analysed.

The use of a generalised scattering technique to model the entire ILC linac is a straightforward and practical way to incorporate machining and alignment errors into the simulation without the necessity to re-mesh the entire geometry. In the present paper the calculations are restricted to the generalised cascaded S matrix technique and redistribution of the frequencies and energy of the modes. The details of the calculation of e.m. fields and associated wake-fields, based on the same generalised scattering matrix technique, will be the subject of a future publication.

REFERENCES

[1] L.Xiao *et al.*, WEPMS048, PAC 2007
[2] G.L. James, IEEE Trans MTT-29, No 10, 1981, p1059
[3] R.M. Jones *et al.*, PAC, Vol 2 p1270, 2003
[4] I.Shinton and R.M.Jones, WEPMN082, PAC 2007
[5] E.Wooldridge and B.Muratori, MOP017,LINAC 2006
[6] S. Molloy *et al.*, Phys Rev Special topics – Accelerators and Beams 9, p112802, 2006,
[7] R. Wanzenberg, TESLA Report 2001-33, 2001.
[8] V.Shemelin SRF070614-02, 2007-10-12
[9] K. Saito *et al.*, KEK private communication
[10] http://lcdev.kek.jp/ILC-AsiaWG/WG5notes
[11] M.Ferrario, TESLA-Report 1993-44
[12] S.A.Kheifets, S.A.Heifets and B.Woo, , IEEE Trans MTT-43, No 6, 1995, p1335
[13] M. Dohlus *et al.*, PAC, Vol 2, p2553, 1997